Talanta 219 (2020) 121202

Contents lists available at ScienceDirect

Talanta

journal homepage: www.elsevier.com/locate/talanta

A visual detection of human immunodeficiency virus gene using ratiometric method enabled by phenol red and target-induced catalytic hairpin assembly

Jiao Zhou, Lei Han, Yu Ling, Lei Wang, Nian Bing Li*, Hong Qun Luo**

School of Chemistry and Chemical Engineering, Southwest University, Chongqing, 400715, People's Republic of China

ARTICLE INFO

Keywords:
Human immunodeficiency virus
Catalytic hairpin assembly
Colorimetric method
Absorbance ratio
Urease

ABSTRACT

Relying on the specific coordination of Ag^+ and mismatched cytosine-cytosine (C–C), the high-efficiency inhibition of urease by Ag^+ ion, and the rapid and sensitive response of phenol red to pH, a sensitive ratiometric sensor has been designed for visual detection of human immunodeficiency virus gene (HIV DNA). This sensor utilizes the HIV DNA to initiate catalytic hairpin assembly (CHA) process, releasing Ag^+ to inhibit subsequent urease-catalyzed urea hydrolysis and prevent the pH of the solution from rising. The CHA process and the absorbance ratio of phenol red at different wavelengths (A_{559}/A_{432}) amplify the signal, allowing the sensor to detect HIV DNA from 10 to 130 nM in a sensitive and highly selective manner with a low detection limit of 7.8 nM. In addition, this sensor can visually distinguish different concentrations of HIV DNA within a certain range and possesses a good recovery in 1% of serum samples, which will provide new ideas for biosensor design, dipstick test, blood test, and other clinical disease prevention.

1. Introduction

Acquired immune deficiency syndrome (AIDS) caused by the human immunodeficiency virus (HIV) is a common infectious disease with high mortality [1,2]. Early detection of AIDS is of great significance for clinical treatment. The clinical diagnostics of AIDS is enzyme-linked immunosorbent assay that possesses high sensitivity and accuracy. However, the enzyme-linked immunosorbent assay takes a long time to produce antibodies, resulting in failure to be detected correctly during the window period, and its operation process is complicated [3,4]. Nucleic acid detection is an effective method for early detection of HIV infection. Regardless of whether the patient is in the window period or not and whether antibodies are produced or not, HIV DNA can be detected in real-time after infection by nucleic acid detection. Therefore, nucleic acid detection has attracted more and more attention in the field of disease diagnosis [4], and different detection methods, such as fluorescence [5,6], electrochemistry [7], colorimetry [8,9], chemiluminescence [10], and surface plasma resonance [11], combined with nanomaterials or nucleic acid amplification methods have been widely used for the specific detection of target DNA. Nevertheless, most of these detection methods require expensive instruments or complicated detection processes, limiting their further application. As a result, the development of convenient and inexpensive sensors is still worth exploring, especially those that can identify HIV DNA with the naked eye or simple instruments [12].

Colorimetric sensors have minimal dependence on detection instruments and the resulting color changes can be recognized by the naked eye [13]. What's more, colorimetry is regarded as a potential strategy in the field of real-time and on-site detection and has been widely used. There are two theories used commonly in colorimetry. One is relying on the localized surface plasmon resonance of precious metal particles, such as gold nanoparticles and silver nanoparticles [14]. The other is depending on the oxidation of small molecules, such as 3, 3′, 5, 5′-tetramethylbenzidine (TMB) [15], 2, 2′-azinobis (3-ethylbenzothiozoline)- 6-sulfonic acid (ABTS) [16], and o-phenylenediamine (OPD) [17]. In addition, the plasmonic colorimetric sensor can be subdivided into three types: One is the aggregation of gold nanoparticles, leading to the color change of the colloid [18,19]. The second is the etching of the metal nanoparticles and the size changes of nanoparticles to produce color changes [14]. The third is to change the shape of the particles by controlling the growth environment, thus causing the changes of color [20–22]. However, precious metal particles are complex in synthesis, expensive in raw materials, poor in dispersibility, and easy to aggregate. In addition, small molecules are prone to self-oxidation over

* Corresponding author.
** Corresponding author.
E-mail addresses: linb@swu.edu.cn (N.B. Li), luohq@swu.edu.cn (H.Q. Luo).

https://doi.org/10.1016/j.talanta.2020.121202
Received 9 January 2020; Received in revised form 18 May 2020; Accepted 20 May 2020
Available online 25 May 2020

time. So, it is necessary to use other cheap and stable molecules to reflect color changes. As a kind of acid-base indicator, phenol red has good stability, responds quickly and sensitively to pH in the range of 6.8–8.4, and has good performance in colorimetric sensing [23,24].

Since the specific coordination between Ag^+ and mismatched cytosine-cytosine (C–C) and Hg^{2+} and mismatched thymidine-thymidine (T-T) has been confirmed [25,26], the probes based on T-Hg^{2+}-T and C–Ag^+-C structures have been widely used in the detection of Hg^{2+} and Ag^+ ions [27,28]. In addition, biosensors based on opening the C–Ag^+-C, T-Hg^{2+}-T hairpin structure, releasing Ag^+ ions and Hg^{2+} ions as output signals have been reported for the detection of proteins, small molecules, and DNA by base complementary pairing or aptamer specific recognition [29–31]. Urease contains a binuclear nickel active site [32] that can catalyze the hydrolysis of urea to form carbon dioxide (CO_2) and ammonia (NH_3), leading to an increase in pH [33]. Moreover, the heavy metal ions, particularly Cu^{2+}, Hg^{2+}, and Ag^+ ions, can bind to thiol groups in the cysteine residue of urease to inhibit urease [32]. Among them, urease is very sensitive to the concentration of Ag^+, and when the concentration of Ag^+ is 2–12 times that of urease, it is sufficient to completely inhibit urease [34].

Based on the highly efficient inhibition of Ag^+ to urease and the fast and sensitive indication of phenol red to pH change, a ratiometric sensor was created for detection of HIV DNA by the naked eye. As shown in Scheme 1, Ag^+ ions are immobilized in the DNA hairpin structure (HP1) by C–Ag^+-C coordination chemistry and cannot inhibit urease activity. Urease catalyzes the hydrolysis of urea, and the produced ammonia raises the pH of the solution. Phenol red indicates a red color, with a strong absorbance at 559 nm and a weak absorbance at 432 nm. When the HIV DNA is present, the hairpin structure can be opened along the sticky end of HP1 and Ag^+ ions are released to inhibit urease. The subsequent urea hydrolysis process cannot occur and the color of the phenol red solution is yellow with a week absorbance at 559 nm and a strong absorbance at 432 nm. What's more, the addition of HP2 allows the target DNA to cycle, achieving a catalytic hairpin assembly (CHA) to signal amplification. With the change of pH, the absorbance of phenol red presents an opposite trend at 559 and 432 nm. Therefore, the absorbance ratio of two wavelengths (A_{559}/A_{432}) is adopted as a signal output to further improve the sensitivity.

2. Experimental

2.1. Materials and instruments

3-Morpholinopropanesulfonic acid (MOPS) and phenol red were offered from Aladdin Reagent Co., Ltd. (Shanghai, China). Urea was obtained from Macklin Co., Ltd (Shanghai, China). Urease and oligonucleotides were purchased from Sangon Co., Ltd. (Shanghai, China). The sequences of the DNA are shown in Table S1 in detail. The other reagents used in this work were of analytical grade and the experimental water was ultrapure water with a resistivity of 18.2 MΩ cm and a pH of 6.0. All of the DNA oligonucleotides were dissolved in MOPS buffer (pH = 6.7) containing 1 mM MOPS, 10 mM $NaNO_3$, and 0.25 mM $Mg(NO_3)_2$, and stored at 4 °C for further use. The healthy human serum was obtained from Southwest University Hospital in Chongqing, China.

UV–vis absorption spectra from 400 to 600 nm were carried out on a UV–vis 2450 spectrophotometer (Shimadzu, Japan).

2.2. Visual detection of HIV DNA

The mixture of HP1 (5 μM, 7 μL) and $AgNO_3$ (1 μM, 7 μL) was denatured at 95 °C for 5 min and cooled to 25 °C in a procedure that drops 1 °C every 2 min to form hairpin structure. After that, 5 μL of target DNA with diverse concentrations, urease (200 nM, 4 μL) and the annealed HP2 (5 μM, 7 μL) were added to the HP1 mixture solution at room temperature for 1 h to release Ag^+ and inhibit the urease activity. Then, phenol red (1 mM, 20 μL) and urea (500 mM, 100 μL) were added to the mixture for color development for 20 min. Finally, the color changes of the solution were recorded on a mobile phone, and the solution was diluted to 500 μL with ultrapure water to record the UV–vis absorption spectra.

2.3. Gel electrophoresis

To verify the progress of the catalytic hairpin assembly (CHA), various samples were analyzed by 15%-native polyacrylamide gel electrophoresis (PAGE). A 15% polyacrylamide gel was prepared by using 40% polyacrylamide and 5 × TBE buffer, and then the sample for loading was prepared by mixing reaction solution (10 μL) with 6 × loading buffer (2 μL). Gel electrophoresis was carried out by incubating in a 1 × TBE buffer at a constant voltage of 80 V for 2 h. Then, the polyacrylamide gel was stained in the gel red dye for 40 min and imaged in a gel imager.

2.4. Application in serum samples

The healthy human serum after centrifugal filtration with an ultrafilter was diluted 100 times and used as a complex actual sample. The detection process was consistent with the section of "Visual detection of HIV DNA", except that the procedure was performed in 1% serum and 5 μL of target DNA solution was replaced by 10 μL of serum solution containing different concentrations of HIV DNA.

3. Results and discussion

3.1. Principle of the analysis

As shown in Scheme 1, HP1 is designed as a hairpin structure with a 6-base sticky end at its 3′ end that can be paired with the target DNA. The stem of HP1 contains a pair of mismatched C–C for binding Ag^+ through C–Ag^+-C coordination. When the target DNA exists, the target DNA opens the hairpin structure along the sticky end of HP1 to form double-stranded DNA (dsDNA), exposing the 5′ end of HP1 and releasing Ag^+ ion. The exposed 5′ end of HP1 can open the hairpin

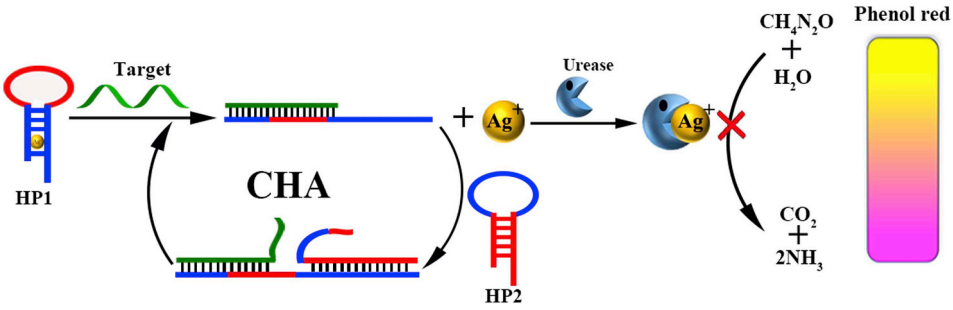

Scheme 1. Schematic diagram of the ratiometric sensor for visual detection of DNA.

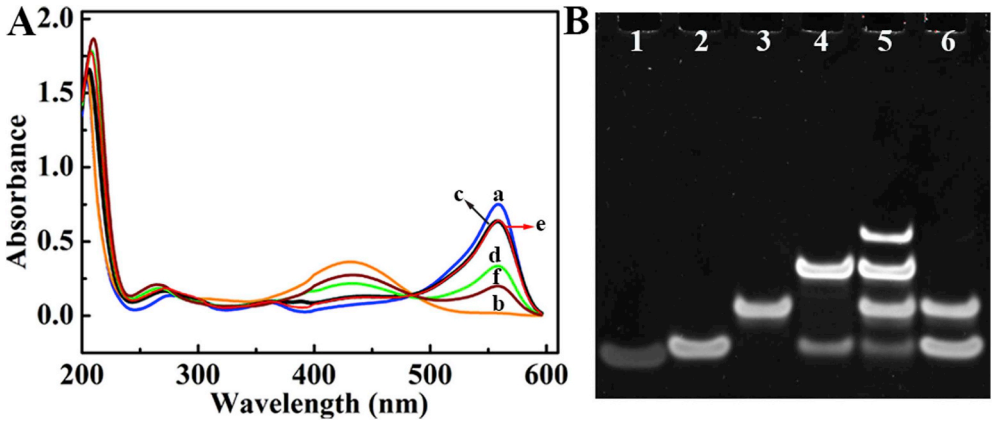

Fig. 1. (A) UV–vis absorption spectra of phenol red solution in different situations. (a) urease + urea, (b) urease + Ag^+ + urea, (c) urease + Ag^+ + HP1 + urea, (d) urease + Ag^+ + HP1 + target + urea, (e) urease + Ag^+ + HP1 + HP2 + urea, (f) urease + Ag^+ + HP1 + target + HP2 + urea. Conditions: 40 μM phenol red, 0.1 M urea, 1.6 nM urease, 14 nM Ag^+, 70 nM HP1, 70 nM HP2, and 80 nM target DNA. (B) Gel images under different conditions (1) HIV DNA, (2) HP1′, (3) HP2′, (4) HIV DNA + HP1′, (5) HIV DNA + HP1′ + HP2′, (6) HP1' + HP2'. (For interpretation of the references to color in this figure legend, the reader is referred to the Web version of this article.)

structure of HP2, and the target DNA paired with HP1 is squeezed out by HP2 to form more stable dsDNA. Therefore, the process of CHA achieves the cycle of the target DNA and amplifies the signal. Moreover, the released Ag^+ ion inhibits urease and prevents urease from catalyzing urea to ammonia and carbon dioxide so that the pH of the solution cannot rise. As a kind of pH indicator, phenol red shows a red color with a characteristic absorption peak at 559 nm when the pH is greater than 7 and shows a yellow color with a characteristic absorption peak at 432 nm when the pH is less than 7. As a result, the color of phenol red changed from red to yellow when the target DNA appeared, the absorbance at 432 nm gradually increased, and the absorbance at 559 nm gradually decreased.

3.2. Feasibility of the strategy

First, for proving the feasibility of this assay, UV–vis absorption spectra under different conditions were recorded. As displayed in Fig. 1A, phenol red shows a strong absorption at 559 nm (curve a), It indicates that urease catalyzes the hydrolysis of urea to produce CO_2 and NH_3, resulting in an increase in pH. After the addition of Ag^+ ions, phenol red exhibits a strong absorption at 432 nm (curve b), showing that Ag^+ ions inhibit the catalytic activity of urease and keep the pH of the solution unchanged. However, Ag^+ is inserted into HP1 through C–Ag^+-C when HP1 is added, so that urease restores activity. Due to the addition of the MOPS buffer solution, the pH change slows down, and the absorbance at 559 nm is slightly lower than that of curve a (curve c). When the target DNA is present, HP1 is opened by target DNA, releasing Ag^+ to inhibit urease activity (curve d). When HP2 is added, the absorbance drops more (curve f), revealing that a CHA reaction occurs and the signal is amplified. In addition, HP1 and HP2 cannot hybridize to release Ag^+ when there is no target DNA (curve e).

Then, the CHA process was verified by gel electrophoresis. Because Ag^+ will chelate with EDTA in the buffer, it affects the electrophoresis results. So, the CHA process was verified by replacing HP1 with HP1′ that without mismatched C–C, and replacing HP2 with HP2′ which is complemented with HP1′ (see the sequence shown in Table S1). As presented in Fig. 1B, lanes 1, 2, and 3 represent the target DNA, HP1′, and HP2′, respectively. A new band with a larger molecular weight produced by hybridization of target DNA and HP1′ appears in lane 4. Compared to lane 4, a larger molecular weight band appears in lane 5, which is the hybrid dsDNA between HP1′ and HP2′. However, no new bands appear in lane 6 when only HP1′ and HP2′ exist, which shows that the two hairpins cannot hybridize to each other.

3.3. Optimization of the detection assay

Several experimental conditions were optimized for the sake of achieving better detection results. By reference to the previous literature [34], 20 min was selected as the time for urea hydrolysis by the catalysis of urease. Then, the minimum concentration of urease required for complete hydrolysis of urea within 20 min was optimized. As shown in Fig. 2A, 1.6 nM urease is sufficient to catalyze the complete hydrolysis of urea (500 mM, 100 μL) and produce a panchromatic change. Fig. 2B shows that at least 14 nM Ag^+ is required to completely inhibit 1.6 nM urease. Due to the limits of the HIV DNA sequence, the sequence of HP1 is fixed. The ratio of HP1 to Ag^+ and the number of mismatched C–C were optimized. As indicated in Fig. 2C, as the concentration of HP1 increases, the more Ag^+ ions are embedded and reach to equilibrium until the concentration ratio of HP1 and Ag^+ is 5:1. Moreover, HP1 containing one mismatched C–C is more effective than HP1-1 containing two mismatched C–C (see the sequence shown in Table S1). This can be explained by that the more complementary bases in the stem of the hairpin, the more stable of the C–Ag^+-C hairpin structure [35]. HP1-1 containing two mismatched C–C and possessing fewer complementary bases is unstable and easy to leak Ag^+, causing high background signal. However, increasing the number of bases in the stem of HP1 will cause the target DNA to turn on HP1 less efficiently. Therefore, HP1 containing one mismatched C–C and HP1: Ag^+ = 5:1 were used in this work. What's more, 1 h was selected as the reaction time of the CHA process, which can be visualized in Fig. 2D.

3.4. Sensitivity of the platform

Under the optimal conditions, the phenol red-based absorbance ratio sensor was used to detect different concentrations of HIV DNA. As displayed in Fig. 3A, the absorbance gradually decreases at 559 nm and gradually increases at 432 nm with the increase of HIV DNA concentration. As presented in Fig. 3B, the ratio value of A_{559}/A_{432} decreases as the concentration of target increases, and has good linearity in the range of 10–60 nM (R^2 = 0.995), and 80–130 nM (R^2 = 0.998). The linear regression equations are Y = −0.0609X + 5.058 and Y = −0.0134X + 1.796, respectively. In the light of 3δ/s (δ represents the standard deviation of the blank sample, and s denotes the slope), the detection limit (LOD) was calculated to be 7.8 nM, and the corresponding value of the LOD was estimated to be about 4.7 × 10^{12} copies/mL. Although the LOD of this platform is not competent for the early stage of HIV infection, our proposed approach exhibits more sensitive or comparable analytical performance compared with some

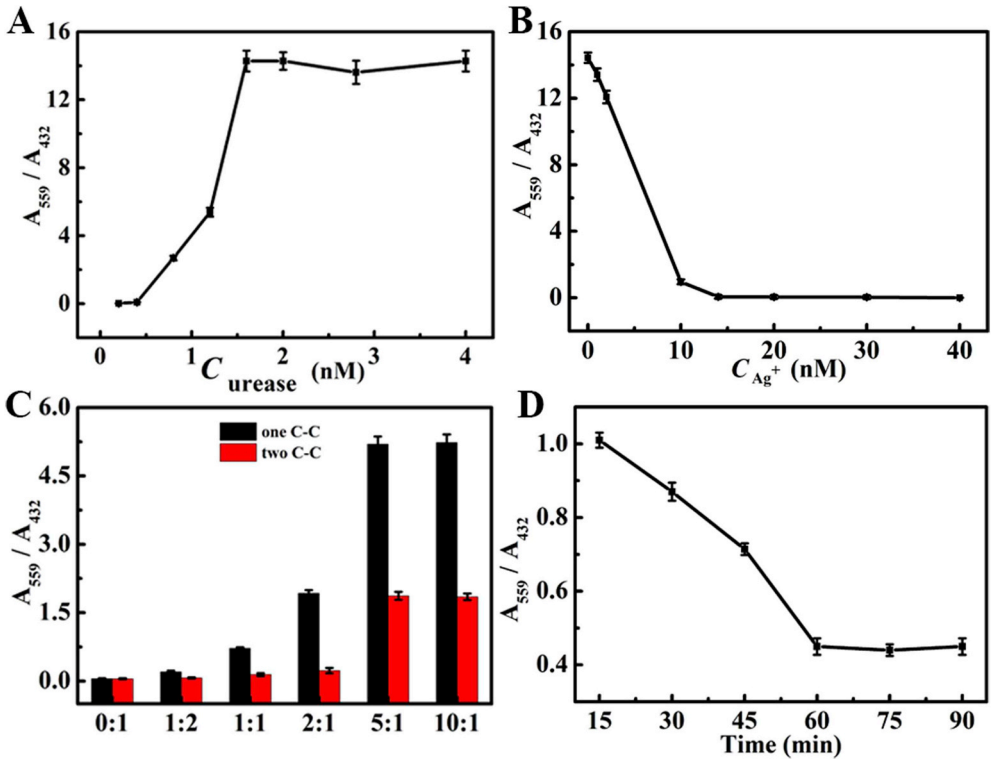

Fig. 2. (A) Effect of different concentrations of urease on the hydrolysis of urea in 20 min. (B) Inhibition of urease by different concentrations of Ag^+. (C) The base optimization of HP1 and the optimization of ratio of HP1 to Ag^+. (D) Optimization of the reaction time of the CHA process. Conditions: 40 μM phenol red, 0.1 M urea, 1.6 nM urease, 14 nM Ag^+, 70 nM HP1, 70 nM HP2, and 100 nM target DNA. (For interpretation of the references to color in this figure legend, the reader is referred to the Web version of this article.)

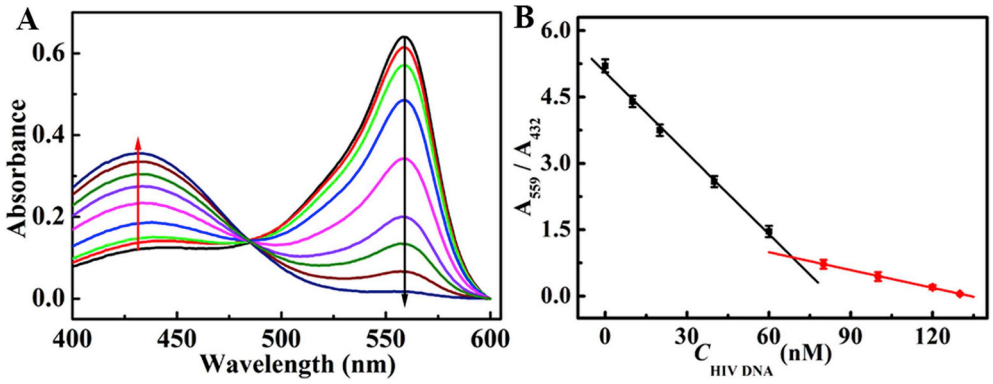

Fig. 3. (A) UV–vis absorption spectra at a variety of HIV DNA from 0 to 130 nM. From top to bottom, the concentration is 0, 10 nM, 20 nM, 40 nM, 60 nM, 80 nM, 100 nM, 120 nM and 130 nM. (B) Linear relationship between the absorbance ratio at 559 nm to 432 nm (A_{559}/A_{432}) and HIV DNA concentration. Conditions: 40 μM phenol red, 0.1 M urea, 1.6 nM urease, 14 nM Ag^+, 70 nM HP1, and 70 nM HP2. (For interpretation of the references to color in this figure legend, the reader is referred to the Web version of this article.)

previous reports of HIV assay (Table S2). What's more, as illustrated in Fig. 4, the color of the solution gradually changes from red to yellow with the increased concentration of HIV DNA. As can be seen from the photo, the color of solution changes significantly and can be distinguished by the naked eyes when the target concentration reaches 40 nM. Until the concentration reaches 130 nM, the color of solution is the same as the color when 14 nM Ag^+ completely inhibits urease. The sensor has good stability within 3 days when stored in the refrigerator at 4 °C (Fig. S1).

Fig. 4. The color change diagram of phenol red solution under different conditions (from left to right are 0, 10, 20, 40, 60, 80, 100, 120, 130 nM HIV DNA and 14 nM Ag^+). (For interpretation of the references to color in this figure legend, the reader is referred to the Web version of this article.)

3.5. Selectivity of the sensor

Single-base mismatched target DNA (1-mis), double-base mismatched target DNA (2-mis), and random DNA sequence (r-DNA) were used to explore the specificity of this sensor for HIV DNA. As depicted in Fig. 5A, the ratio value of A_{559}/A_{432} in the 1-mis group is slightly lower than that in the blank group, and the 2-mis group and the r-DNA group are consistent with the background group, while the target group is significantly decreased at the same concentration. This demonstrates that the sensor has good selectivity for the target DNA and is capable of distinguishing single-base mismatched DNA. At the same time, as can be seen from the gel imaging diagram in Fig. 5B, no new bands appear from lanes 3 to 8. This indicates that even a single-base mismatched target DNA cannot open HP1′ and the CHA process does not occur, which also demonstrates that the sensor has specific recognition ability

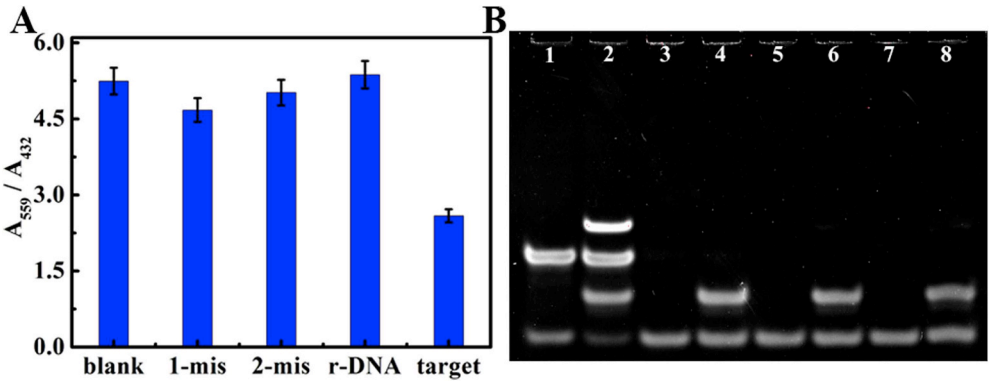

Fig. 5. (A) Selective studies of this sensor for HIV DNA with different mismatch conditions. (from left to right, there are blank groups, single base mismatches, double base mismatches, random DNA sequence, and target groups.) Conditions: the target DNA concentrations of all groups were 40 nM. (B) The gel imaging diagram of the CHA process with different mismatch conditions (1) HIV DNA + HP1′ (2) HIV DNA + HP1′ + HP2′ (3) single base mismatches-HIV DNA + HP1′, (4) single base mismatches-HIV DNA + HP1′ + HP2′, (5) double base mismatches-HIV DNA + HP1′, (6) double base mismatches-HIV DNA + HP1′ + HP2′, (7) random DNA sequence + HP1′, (8) random DNA sequence + HP1′ + HP2'.

Table 1
Analysis of HIV DNA in 1% of serum sample (n = 3).

Number	Added (nM)	Detected (nM)	Recovery (%)	RSD (%)
1	0	Not found	/	2.33
2	10	11.34	113.40	1.11
3	80	89.10	111.38	3.37
4	120	117.79	98.16	1.55

for the target DNA.

3.6. Recovery analysis of HIV DNA in serum samples

The method we proposed yielded satisfactory results in 1% of healthy human serum samples. As shown in Table 1, the recovery of the three different concentrations of HIV DNA ranges from 98.16% to 113.40%, and the relative standard deviation is between 1.11% and 3.37%, proving that the method has good reproducibility, which can be used in complex biological samples and providing a new idea for blood routine examination.

4. Conclusion

In summary, a ratiometric absorbance sensor has been developed for visual detection of HIV DNA. The sensor used the HIV DNA to open the hairpin DNA to adjust the degree of inhibition of urease by Ag^+, and the sensitive response of phenol red to pH change produced by urease-specific catalytic hydrolysis of urea as an output signal of the ratio sensor. Thanks to the CHA process and the absorbance ratio of phenol red at different wavelengths, the signal has been amplified synergistically, making the sensor have higher sensitivity. What's more, unlike other visual sensors, this sensor is based on the indicator's response to changing the pH value of urea hydrolysis catalyzed by urease, which not only does not require a complex synthesis process, does not undergo an auto-oxidation process, but also has high efficiency and rapidity of enzymatic reaction. Moreover, the system has a good recovery for HIV DNA detection in serum samples, provides a new idea for visual AIDS blood testing, and has potential in point-of-care testing.

CRediT authorship contribution statement

Jiao Zhou: Conceptualization, Methodology, Investigation, Writing - original draft. **Lei Han:** Investigation, Validation. **Yu Ling:** Resources, Investigation. **Lei Wang:** Visualization, Formal analysis. **Nian Bing Li:** Supervision, Project administration, Data curation, Funding acquisition. **Hong Qun Luo:** Conceptualization, Resources, Project administration, Writing - review & editing.

Declaration of competing interest

The authors declare that they have no known competing financial interests or personal relationships that could have appeared to influence the work reported in this paper.

Acknowledgments

The authors sincerely acknowledge the support of the National Natural Science Foundation of China (No. 21675131), and the Natural Science Foundation of Chongqing (No. CSTC-2015jcyjB50001).

Appendix A. Supplementary data

Supplementary data to this article can be found online at https://doi.org/10.1016/j.talanta.2020.121202.

References

[1] B. Babamiri, A. Salimi, R. Hallaj, A molecularly imprinted electrochemiluminescence sensor for ultrasensitive HIV-1 gene detection using EuS nanocrystals as luminophore, Biosens. Bioelectron. 117 (2018) 332–339.
[2] Y. Zhou, Y. Chen, H. He, J. Liao, H.T.T. Duong, M. Parviz, D. Jin, A homogeneous DNA assay by recovering inhibited emission of rare earth ions-doped upconversion nanoparticles, J. Rare Earths 37 (2019) 11–18.
[3] N. Aroonyadet, X. Wang, Y. Song, H. Chen, R.J. Cote, M.E. Thompson, R.H. Datar, C. Zhou, Highly scalable, uniform, and sensitive biosensors based on top-down indium oxide nanoribbons and electronic enzyme-linked immunosorbent assay, Nano Lett 15 (2015) 1943–1951.
[4] K. Wang, D. Fan, Y. Liu, S. Dong, Cascaded multiple amplification strategy for ultrasensitive detection of HIV/HCV virus DNA, Biosens. Bioelectron. 87 (2017) 116–121.
[5] Y.D. Ye, L. Xia, D.D. Xu, X.J. Xing, D.W. Pang, H.W. Tang, DNA-stabilized silver nanoclusters and carbon nanoparticles oxide: a sensitive platform for label-free fluorescence turn-on detection of HIV-DNA sequences, Biosens. Bioelectron. 85 (2016) 837–843.
[6] J. Zheng, X. Ji, M. Du, S. Tian, Z. He, Rational construction of a DNA nanomachine for HIV nucleic acid ultrasensitive sensing, Nanoscale 10 (2018) 17206–17211.
[7] C. Tao, Y. Yan, H. Xiang, D. Zhu, W. Cheng, H. Ju, S. Ding, A new mode for highly sensitive and specific detection of DNA based on exonuclease III-assisted target recycling amplification and mismatched catalytic hairpin assembly, Chem. Commun. 51 (2015) 4220–4222.
[8] Z. Zhou, W. Wei, Y. Zhang, S. Liu, DNA-responsive disassembly of AuNP aggregates: influence of nonbase-paired regions and colorimetric DNA detection by exonuclease III aided amplification, J. Mater. Chem. B 1 (2013) 2851.
[9] Q. Liu, L. Li, Y. Zhao, Z. Chen, Colorimetric detection of DNA at the nanomolar level based on enzyme-induced gold nanoparticle de-aggregation, Microchim. Acta 185 (2018) 301.
[10] R. Freeman, X. Liu, I. Willner, Chemiluminescent and chemiluminescence resonance energy transfer (CRET) detection of DNA, metal ions, and aptamer–substrate complexes using hemin/G-quadruplexes and CdSe/ZnS quantum dots, J. Am. Chem. Soc. 133 (2011) 11597–11604.
[11] J. Spadavecchia, A. Barras, J. Lyskawa, P. Woisel, W. Laure, C.M. Pradier, R. Boukherroub, S. Szunerits, Approach for plasmonic based DNA sensing: amplification of the wavelength shift and simultaneous detection of the plasmon modes of gold nanostructures, Anal. Chem. 85 (2013) 3288–3296.
[12] W. Zhou, X. Gong, Y. Xiang, R. Yuan, Y. Chai, Quadratic recycling amplification for

label-free and sensitive visual detection of HIV DNA, Biosens. Bioelectron. 55 (2014) 220–224.
[13] N. Hao, J. Lu, Z. Zhou, R. Hua, K. Wang, A pH-resolved colorimetric biosensor for simultaneous multiple target detection, ACS Sens 3 (2018) 2159–2165.
[14] Z. Zhang, H. Wang, Z. Chen, X. Wang, J. Choo, L. Chen, Plasmonic colorimetric sensors based on etching and growth of noble metal nanoparticles: strategies and applications, Biosens. Bioelectron. 114 (2018) 52–65.
[15] S. Zhang, H. Li, Z. Wang, J. Liu, H. Zhang, B. Wang, Z. Yang, A strongly coupled Au/Fe_3O_4/GO hybrid material with enhanced nanozyme activity for highly sensitive colorimetric detection, and rapid and efficient removal of Hg^{2+} in aqueous solutions, Nanoscale 7 (2015) 8495–8502.
[16] J. Li, Q.H. Yao, H.E. Fu, X.L. Zhang, H.H. Yang, High sensitive and label-free colorimetric DNA detection based on nicking endonuclease-assisted activation of DNAzymes, Talanta 85 (2011) 91–96.
[17] F. Li, J. Liu, Y. Hu, N. Deng, J. He, An ultrasensitive label-free colorimetric assay for glutathione based on Ag^+ regulated autocatalytic oxidation of o-phenylenediamine, Talanta 186 (2018) 330–336.
[18] Z. Huang, J. Chen, Z. Luo, X. Wang, Y. Duan, Label-free and enzyme-free colorimetric detection of Pb^{2+} based on RNA cleavage and annealing-accelerated hybridization chain reaction, Anal. Chem. 91 (2019) 4806–4813.
[19] P. Liu, X. Yang, S. Sun, Q. Wang, K. Wang, J. Huang, J. Liu, L. He, Enzyme-free colorimetric detection of DNA by using gold nanoparticles and hybridization chain reaction amplification, Anal. Chem. 85 (2013) 7689–7695.
[20] T. Lin, Y. Wu, Z. Li, Z. Song, L. Guo, F. Fu, Visual monitoring of food spoilage based on hydrolysis-induced silver metallization of Au nanorods, Anal. Chem. 88 (2016) 11022–11027.
[21] S. Lu, X. Zhang, L. Chen, P. Yang, Colorimetric visualization of superoxide dismutase in serum via etching of Au nanorods from superoxide radical, Sens Actuators B Chem 259 (2018) 1066–1072.
[22] D. Wang, R. Guo, Y. Wei, Y. Zhang, X. Zhao, Z. Xu, Sensitive multicolor visual detection of telomerase activity based on catalytic hairpin assembly and etching of Au nanorods, Biosens. Bioelectron. 122 (2018) 247–253.
[23] S.V. Hamidi, J. Perreault, Simple rolling circle amplification colorimetric assay based on pH for target DNA detection, Talanta 201 (2019) 419–425.
[24] L. He, Y. Lu, F. Wang, X. Gao, Y. Chen, Y. Liu, Bare eye detection of Hg(II) ions based on enzyme inhibition and using mercaptoethanol as a reagent to improve selectivity, Microchim. Acta 185 (2018) 174.
[25] Y. Miyake, H. Togashi, M. Tashiro, H. Yamaguchi, S. Oda, M. Kudo, Y. Tanaka, Y. Kondo, R. Sawa, T. Fujimoto, T. Machinami, A. Ono, Mercury^{II}-mediated formation of thymine-Hg^{II}-thymine base pairs in DNA duplexes, J. Am. Chem. Soc. 128 (2006) 2172–2173.
[26] A. Ono, S. Cao, H. Togashi, M. Tashiro, T. Fujimoto, T. Machinami, S. Oda, Y. Miyake, I. Okamoto, Y. Tanaka, Specific interactions between silver(i) ions and cytosine–cytosine pairs in DNA duplexes, Chem. Commun. (2008) 4825–4827.
[27] G.L. Li, Z.S. Zhao, J.Y. Liu, G.B. Jiang, Effective heavy metal removal from aqueous systems by thiol functionalized magnetic mesoporous silica, J. Hazard. Mater. 192 (2011) 277–283.
[28] J. Li, H. Xi, C. Kong, Q. Liu, Z. Chen, "Aggregation-to-deaggregation" colorimetric signal amplification strategy for Ag^+ detection at the femtomolar level with dark-field microscope observation, Anal. Chem. 90 (2018) 11723–11727.
[29] P. Chen, E. Sawyer, K. Sun, X. Zhang, C. Chen, B. Ying, X. Wei, Z. Wu, J. Geng, A general strategy for label-free homogeneous bioassays based on selective recognition and silver ion-mediated conformational switch, Talanta 201 (2019) 9–15.
[30] P. Chen, P. Wu, Y. Zhang, J. Chen, X. Jiang, C. Zheng, X. Hou, Strand displacement-induced enzyme-free amplification for label-free and separation-free ultrasensitive atomic fluorescence spectrometric detection of nucleic acids and proteins, Anal. Chem. 88 (2016) 12386–12392.
[31] A.L. Sun, K. Deng, W.L. Fu, Exonuclease III-based target recycling for ultrasensitive homogeneous monitoring of HIV DNA using Ag^+-coordinated hairpin probe, Biosens. Bioelectron. 74 (2015) 66–70.
[32] B. Krajewska, Mono- (Ag, Hg) and di- (Cu, Hg) valent metal ions effects on the activity of jack bean urease. Probing the modes of metal binding to the enzyme, J. Enzyme Inhib. Med. Chem. 23 (2008) 535–542.
[33] L. Mazzei, M. Cianci, A. Gonzalez Vara, S. Ciurli, The structure of urease inactivated by Ag(i): a new paradigm for enzyme inhibition by heavy metals, Dalton Trans 47 (2018) 8240–8247.
[34] M.G. Wolfe, M.M. Ali, J.D. Brennan, Enzymatic litmus test for selective colorimetric detection of C–C single nucleotide polymorphisms, Anal. Chem. 91 (2019) 4735–4740.
[35] H. Wang, H. Yin, H. Huang, K. Li, Y. Zhou, G.I.N. Waterhouse, H. Lin, S. Ai, Dual-signal amplified photoelectrochemical biosensor for detection of N^6-methyladenosine based on $BiVO_4$-110-TiO_2 heterojunction, Ag^+-mediated cytosine pairs, Biosens. Bioelectron. 108 (2018) 89–96.